250693

DP-MS-87-77

# POURBAIX DIAGRAM FOR THE PREDICTION OF WASTE GLASS DURABILITY IN GEOLOGIC ENVIRONMENTS

C. M. Jantzen
E. I. du Pont de Nemours & Co.
Savannah River Laboratory
Aiken, SC 29808

SRL
RECORD COPY

A paper proposed for presentation at the
Materials Research Society XI International Symposium
on the Scientific Basis for Nuclear Waste Management
Boston, Massachussetts
December 3, 1987

and for publication in the proceedings

---

This paper was prepared in connection with work done under Contract No. DE-AC09-76SR00001 with the U.S. Department of Energy. By acceptance of this paper, the publisher and /or recipient acknowledges the U.S. Government's right to retain a nonexclusive, royalty-free license in and to any copyright covering this paper, along with the right to reproduce and to authorize others to reproduce all or part of the copyrighted paper.

TO BE PUBLISHED IN
Scientific Basis for Nuclear Waste Management, XI
M.J. Apted and R.E. Westerman (Eds) 1988

# POURBAIX DIAGRAM FOR THE PREDICTION OF WASTE GLASS DURABILITY IN GEOLOGIC ENVIRONMENTS

CAROL M. JANTZEN
E. I. du Pont de Nemours & Company. Savannah River Laboratory.
Aiken, South Carolina 29808

## ABSTRACT

Dissolution of nuclear waste glass occurs by corrosion mechanisms similar to those of metallurgical and mineralogic systems albeit on different time scales. The effects of imposed pH and oxidation potential (Eh) conditions existing in natural environments on metals and minerals have been quantatively and phenomenologically described in compendiums of Pourbaix (pH-potential) diagrams. Construction of Pourbaix diagrams to quantify the response of nuclear waste glasses to repository specific pH and Eh conditions is demonstrated. The expected long-term effects of groundwater contact on the durability of nuclear waste glasses can then be unified.

## INTRODUCTION

To predict the long-term effects of groundwater contact on nuclear waste glass durability, the detailed nature of the dissolution process and the durability of the glass as a function of the solution pH and oxidation potential (Eh) must be understood. During dissolution in aqueous environments, nuclear waste glasses exhibit corrosion phenomena similar to metallurgical systems albeit on different time scales. For storage of nuclear waste glass, we are concerned with mechanisms that take place over thousands of years. Glasses undergo active dissolution, passivation due to surface layer formation, and immunity (the state of a solid in which dissolution is thermodynamically impossible). The particular corrosion phenomena observed is dependent on the pH and Eh of the aqueous environment.

The effects of aqueous environments on metallurgical corrosion have been described by Pourbaix [1] in an Atlas of equilibrium pH-electrochemical potential (Eh) diagrams. Pourbaix diagrams have also been constructed to assess mineral stability during exposure to the environment [2], e.g. weathering. Construction of Pourbaix diagrams for glass dissolution would conceptually unify the dissolution behavior of all glasses as a function of pH-Eh conditions imposed in natural environments, e.g. weathering and/or groundwater exposure. In particular, Pourbaix diagrams are applicable to the response of borosilicate nuclear waste glasses to the complex groundwaters in a geologic repository.

The relative durabilities of over 300 natural and man-made glasses have been compared [3-6] based on their relative thermodynamic stabilities, expressed as the free energies of hydration, $\Delta G_{hyd}$. Linear relationships have been determined between the logarithmic extent of hydration (log $NL_{Si}$ or $NL_B$ in grams of glass per square meter of glass surface area), the pH, and the calculated $\Delta G_{hyd}$ for glass dissolution in deionized water [7]. The fundamental thermodynamic relationship between $\Delta G_{hyd}$ and pH can be determined from the Nernst equation. The relationship between log $NL_{Si}$ (or log $NL_B$) and pH is determined by the pH dependence of the ion activities [7]. The relationship between $\Delta G_{hyd}$ and the solution Eh can also be defined from the Nernst equation [7].

In this study, the relationships between pH-$\Delta G_{hyd}$, pH-log($NL_{Si}$), and pH-log($NL_B$) are used to quantify a Pourbaix diagram for nuclear waste glass. The known effects of pH and Eh on glass dissolution and surface layer formation are used to define the thermodynamically calculated phase stability fields. The use of the Pourbaix diagram to predict the performance of nuclear waste glass in repository environments is discussed.

## THEORETICAL

### Pourbaix Diagrams

Equilibrium pH-electrochemical potential (E or Eh) diagrams were developed by Pourbaix [1] to describe the effects of aqueous environments on corrosion of metals. Pourbaix diagrams are use in geochemistry and referred to as pH-Eh diagrams. These diagrams are also used to depict the stability relations among solid phases [8,9] and to assess mineral (rock) stability during weathering [2]. In pedology, pH-potential diagrams, referenced as pH-pe (pe = 16.9 Eh at 25°C) diagrams, are used to examine soil diagenesis and soil chemistry. The processes of rock weathering and soil formation are derived from the superimposition of the dilute, acidic, and oxidizing solutions of the earth's surface environment upon the mineral species which formed under high-temperature reducing conditions below the earth's surface [10]. These mineral species and intergranular glasses have been in contact with concentrated, alkaline, and oxygen-free (reducing) sub-surface aqueous environments for millions of years without undergoing alteration [10]. (Hanford basalts can contain up to 60 volume percent intergranular glass). This is analogous to the corrosion of metals formed under high-temperature reducing conditions and then exposed to the varied environments of the earth's surface [10]. Extending the analogy, the geologic performance of radioactive waste glass fabricated under high-temperature reducing conditions [11,12] with concentrated alkaline to neutral reducing groundwaters anticipated in a geologic repository can be understood.

By definition, all aqueous solutions contain water and, hence, the thermodynamic stability of water defines the boundary conditions for all pH-potential diagrams. The upper limit of water stability is defined by the oxidizing potential necessary to decompose water to oxygen while the lower limit of water stability is defined by the reducing potential necessary to decompose water to hydrogen. All Eh-pH dependent equilibria, including the upper and lower stability limits of water, are defined from thermodynamic equilibria by the Nernst equation

$$Eh = E^\circ + \frac{RT}{n\mathcal{F}} \ln \frac{[\text{oxidized state}]}{[\text{reduced state}]} \qquad (1a)$$

where

- $E^\circ$ = the voltage (EMF) of a reaction when all substances involved are at unit activity
- $E^\circ = \Delta F^\circ_r / n\mathcal{F}$
- $n$ = number of electrons transferred
- $R$ = the gas constant ($1.987 \times 10^{-3}$ Kcal/deg)
- $\mathcal{F}$ = the Faraday constant (23.06 Kcal/volt-gram equivalent)
- $T$ = temperature in °K
- $[\ ]$ = ion activities

At 25°C, for equilibria which are both Eh and pH dependent, this reduces to

$$Eh = E^\circ - \frac{0.059}{n}\, pH \qquad (1b)$$

The upper and lower stability limits of water have slopes of -0.059 (at 25°C) and an intercept of $E^\circ$ defined from Equation 1b. Eh independent reactions parallel the Eh axis and pH independent reactions parallel the pH axis.

Activity-pH (or activity-Eh) diagrams provide the fundamental correlation between ion concentrations in solution and the free energy of a hydration reaction (Equation 1a). Solubility concentrations differ from the activities by a factor, $\gamma$, known as the activity coefficient [2]. If $\gamma$ is approximately equal to one then the ion activity approximately equals the

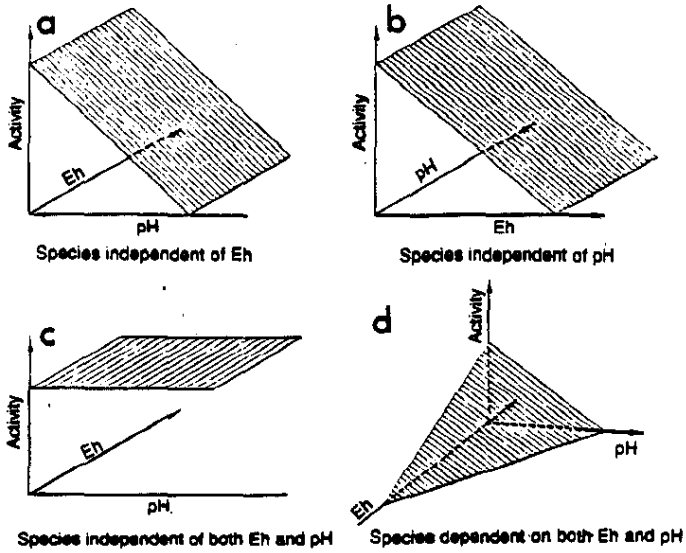


Figure 1 Three dimensional representation of the relations between the ion activity of a species, solution Eh and pH (after Krumbein and Garrels[9]).

ion concentration. The factor $\gamma$ is dependent on the ionic strength of the solution and is a function of the multiple hydration, ionization, and complexation reactions that the ion participates in. However, the activity-pH diagrams provide the fundamental correlation between minimum solubility of an ion in solution and the free energy [2,13]. The interrelation of activity (concentration), pH, and Eh is shown schematically in Figure 1 for species which are

- independent of Eh
- independent of pH
- independent of both Eh and pH
- dependent on both Eh and pH.

The influence of pH on the activity of vitreous silica can be thermodynamically calculated from the equilibrium constants for the hydration of $SiO_2$ to silicic acid and the equilibrium constants for silicic acid dissociation [1,14]. Likewise, the activity-pH relations for vitreous $B_2O_3$ hydration can be calculated from the equilibrium constants for the hydration of vitreous $B_2O_3$ to boric acid and the equilibrium constants for boric acid dissociation [7]. The hydration of vitreous silica (or vitreous boric oxide) is independent of Eh and hence, the activity-pH diagrams provide the fundamental correlation between silica (or boron) concentration in solution and the free energy. Silicon and boron concentration dependent contours would, therefore, parallel the Eh axis as shown in Figure 1a [1, 7].

If the dissolution of silicate and borosilicate glasses can be described by the activity diagram for the dissolution of amorphous silica as suggested by Grambow [15,16], then one Pourbaix diagram may describe the environmental response of all silicate and borosilicate glasses fabricated under high-temperature oxidizing or reducing conditions. This relation is supported by the data Reimus of [17] which indicates that the aqueous solution activities for a range of nuclear waste glasses are all approximately the same because many of the dissolved species are at their solubility limit. A second order effect of the aqueous solution redox interactions with glasses fabricated under high-temperature reducing conditions and containing redox active species would then be to alter the driving force for dissolution.

Hydration Thermodynamics

The free energy of hydration is calculated from the glass composition [18] and the final solution pH [6]. During glass dissolution in deionized water, the species released from the glass were found to control the leachate pH, e.g the solution pH can be calculated from speciation as shown by Grambow [15]. In groundwater leachants, however, the pH was found to be controlled by the buffering capacity of the groundwater. The data for glass dissolution in silicate groundwaters superimposes on the linear relationship defined by glass dissolution in deionized water [19]. The glass durability can, therefore, be predicted from the glass composition and the groundwater pH.

## EXPERIMENTAL PROCEDURES

The durability of glass and glass-ceramic monoliths were determined using the Materials Characterization Center (MCC-1) test procedure [20]. The leachant was deionized water, the test duration was 28 days, and the test temperature was 90°C. Details of the experimental and analytic procedures are given elsewhere [5-7].

## QUANTIFICATION OF A POURBAIX DIAGRAM FOR GLASS

For over 300 individual glass durability tests, regression equations were statistically calculated [7] for binary combinations of the following variables: $\Delta G_{hyd}$, $\log(NL_{Si})$, $\log(NL_B)$, and $-\log(H^+)$ or pH. Several regressors were found to be nearly linear combinations of other regressors in the data base, e.g. colinear. The variables (n=4) were examined in n-1 combinations. Combinations of n-1 variables have three degrees of freedom. However, the three degrees of freedom are limited by the strong variable pair interactions between $\Delta G_{hyd}$-pH, $\log(NL_{Si})$-pH, and $\log(NL_B)$-pH [7]. The variable pair interactions impart an additional restriction on any n-1 combination so that the degrees of freedom is reduced to n-2 or 2.

The colinearity between the regressors is caused by the fundamental thermodynamic relationships among $\Delta G_{hyd}$, the solution pH, and the concentration of species in solution. The $\log(NL_{Si})$, $\Delta G_{hyd}$, and the pH are highly colinear because the pH and $\Delta G_{hyd}$ are related through the Nernst equation [7]. In addition, $\log(NL_{Si})$ is related to the pH through the activity-pH relationship. The $\log(NL_{Si})$, $\log(NL_B)$, and the pH are highly colinear because of the restriction imposed by congruent dissolution [7]. Each of these solution species is colinear with pH because of the pH dependence of the ion activities. The $\log(NL_{Si})$ and $\log(NL_B)$ are related to $\Delta G_{hyd}$ through the equilibrium constants for the hydration of $SiO_2$ and $B_2O_3$ and the equilibrium constants for silicic acid and boric acid dissociation. Therefore, combinations of the following n-1 variables can be defined by the slopes between the binary pairs of variables given below:

- $\log(NL_{Si}) - \Delta G_{hyd} - pH$
- $\log(NL_B) - \Delta G_{hyd} - pH$
- $\Delta G_{hyd} - \log(NL_{Si}) - \log(NL_B)$
- $pH - \log(NL_{Si}) - \log(NL_B)$

Over the limited pH range (~5-13 pH) of the deionized water experiments, the statistically determined slopes between pH and the remaining three variables gave [7] the following:

$$pH = -0.489\,\Delta G_{hyd} + 6.12 \quad (2)$$

$$\log(NL_{Si}) = +0.429\,pH - 2.73 \quad (3)$$

$$\log(NL_{B}) = +0.416\,pH - 2.31 \quad (4)$$

Because of the colinearity relationships between pH-log($NL_{Si}$) and pH-log($NL_B$), a three dimensional Eh-pH-concentration diagram similar to the schematic Eh-pH-activity diagram in Figure 1 can be constructed. The concentrations of Si and B in solution have been shown experimentally [21,22] to be almost completely independent of the solution Eh. The Eh independent equilibria will, therefore, parallel the Eh axis as shown schematically in Figure 1a. Isopleths of constant solution concentration can be contoured on the Eh-pH plane from the statistically determined slopes given in Equations 3 and 4. A quantative Pourbaix diagram for glass dissolution can, therefore, be developed (Figure 2a and 2b).

Because of the relation of $\Delta G_{hyd}$ to Eh and pH through the Nernst equation [7] and the colinearity of $\Delta G_{hyd}$ to pH, a similar three dimensional Eh-pH-$\Delta G_{hyd}$ diagram can be derived. Since $\Delta G_{hyd}$ was theoretically shown [7] to be relatively insensitive to solution Eh, it can also be contoured parallel to the Eh axis on a Pourbaix diagram for glass (Figure 2c). The statistically determined $\Delta G_{hyd}$-pH slope given in Equation 2 is used to determine the contour interval.

## DETERMINATION OF THE POURBAIX DIAGRAM STABILITY FIELDS

The data of Adams [23], Wicks [24] and others [25] (Table 1) indicates that high silica commercial glasses, and low silica glasses including borosilicate glasses undergo primary network dissolution at pH ~10. This pH corresponds to the calculated Eh-independent boundaries between $H_2SiO_3/HSiO_3^-$ and $H_3BO_3/H_2BO_3^-$. The pH of the $H_2SiO_3/HSiO_3^-$ boundary is chosen as representative of the alkaline network dissolution boundary for the regime of active corrosion on a Pourbaix diagram for glass (Figure 3a). The boundary plotted corresponds to log C = $10^{-4}$M $H_2SiO_4$.

The data of Adams [23] indicates that high-silica commercial glasses do not undergo active corrosion in acidic media as do lower silica content glasses (Table 1), including nuclear waste glasses [23,25]. The low-silica-containing glasses follow parabolic relationships with solution pH [23-26]. In order to describe a generalized Pourbaix diagram for these glasses, the Eh-independent acidic stability field for active glass dissolution is chosen (Figure 3a) as the pH of the zero point of charge (ZPC). The zeta potential-pH response for vitreous silica, borosilicate glass, soda-lime-silica glass and soda aluminosilicate glass are all similar [27] and the ZPC for all these glasses is ~2 (Table 1). Horn and Onada [27] attribute the similarity of the zeta potential-pH response of these compositionally diverse glasses to the dominant role of the silica network and the minimal role of the network modifying cations. Indeed, the ZPC of SRP borosilicate nuclear waste glass was measured as exactly 2 (Figure 4). Due to the wide range of glass compositions that have a ZPC of ~2, this pH value is chosen as the approximate boundary for the stability field of active corrosion on the Pourbaix diagram.

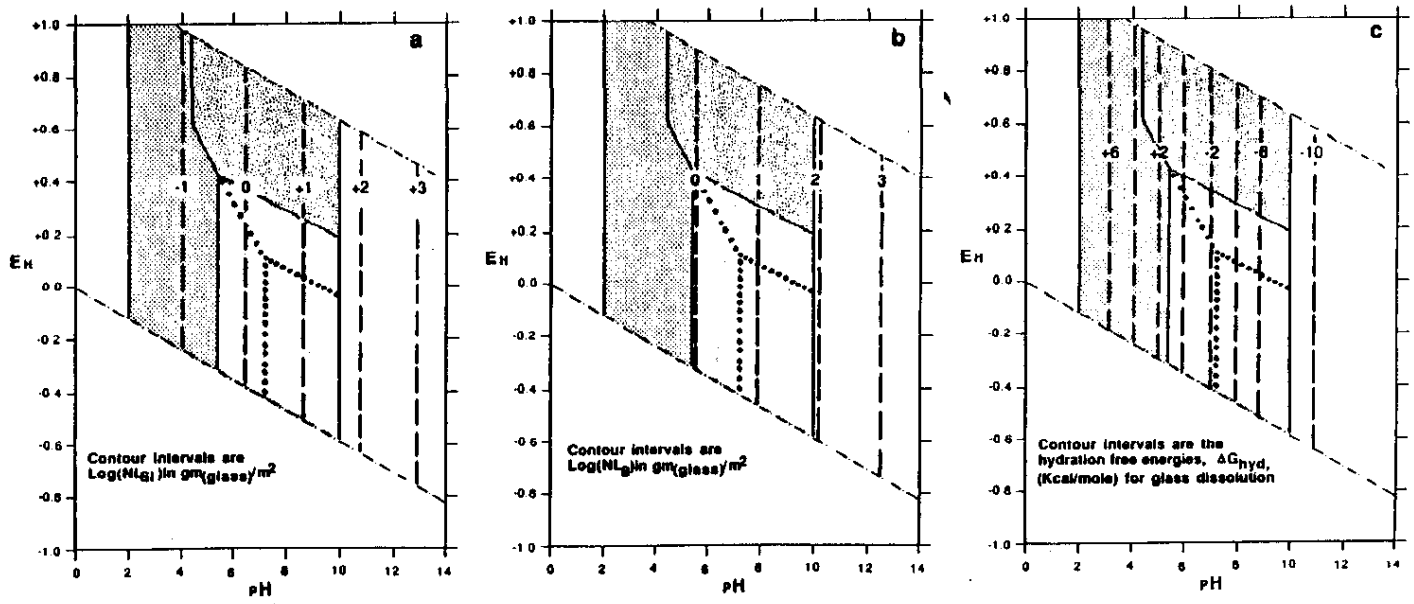


Figure 2 Pourbaix diagrams for glass dissolution based on release of silicon and boron to solution and on the hydration free energy, $\Delta G_{hyd}$. Contours represent Eh independent-pH dependent variables for the over 300 glasses studied. Contour intervals determined from the slopes given in Equations 2-4 only apply over the pH range ~5-13.

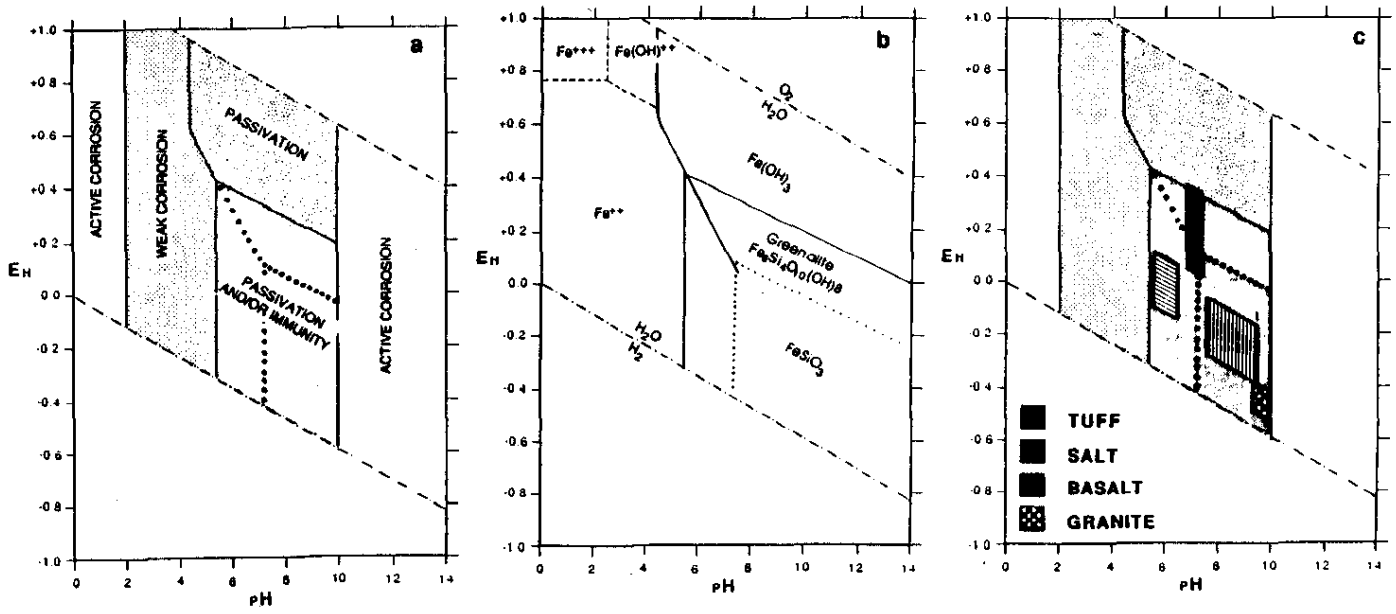


Figure 3 (a) The Pourbaix diagram for low silica and borosilicate glasses. Note this diagram can be used quantatively to predict glass dissolution by superimposition of the contours shown in Figure 2.
(b) Phase stability fields used in the determination of the Pourbaix diagram. The determination of the thermodynamically calculated phase stability fields is discussed in the text.
(c) The Pourbaix diagram of Figure 5a showing that glass dissolution under the anticipated groundwater conditons of a geologic repository will be controlled by glass surface layer passivation and/or thermodynamic immunity.

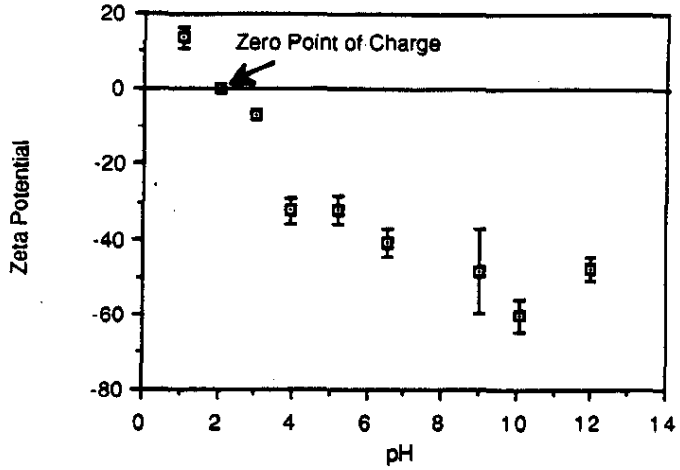


Figure 4 The pH of the zero point of charge (ZPC), $pH_{ZPC}$, for SRP 165 waste glass (pH ~2).

At pH values between 2 and 10 in oxidizing environments, hydrolysis of glass occurs by nucleophilic attack. The glass surface charges are negative and surface layer formation occurs by reprecipitation or chemisorption [28] of metal hydroxides (which are positively charged) from solution. For example, $Al(OH)_3$ and $Fe(OH)_3$ are the predominant metal hydroxide species between pH values of ~3-11 and ~3-13 respectively [29]. Both $Al(OH)_3$ and $Fe(OH)_3$ have been reported [5,24,30,31] as primary components of surface layers observed on leached glasses containing $Al_2O_3$ and $Fe_2O_3$. The presence of $Al_2O_3$ and $Fe_2O_3$ in glasses is known [29] to increase its durability in the pH range of 4 to 9, indicating that the surface layer formation observed on such glasses is passivating as indicated mechanistically by Wicks [24] and others [30,32,33].

Table 1. Regions of Active Corrosion, Passivation, and Immunity for Glass

| Solution | Glass | pH | Eh | Observation | Reference |
|---|---|---|---|---|---|
| DI Water | Waste | <6 | Oxic | Active Corrosion | 24 |
| DI Water | Waste | 6-8.5 | Oxic | Minimal Corrosion Surface Layer Formation | 24 |
| DI Water | Waste | 8.5-11 | Oxic | Active Corrosion, Some Layer Formation | 24 |
| pH Buffers | Waste | 5-9 | Oxic | Minimal Corrosion | 26 |
| pH Buffers | Waste | <3 | Oxic | No Layer Formation | 26 |
| pH 3 Buffer | Waste | 3 | Oxic | Active Corrosion | 26 |
| pH 7 Buffer | Waste | 7 | Oxic | Layer Formation | 26 |
| pH 11 Buffer | Waste | 11 | Oxic | Poor Layer Formation | 26 |
| DI Water | SLS* | 7-9 | Oxic | Minimal Corrosion | 25 |
| DI Water | SLS | 9-11 | Oxic | Active Corrosion | 25 |
| DI Water | Waste | 7-9 | Oxic | Corrosion Controlled by $Fe(OH)_3$ | 31 |
| DI Water | Waste | 7-9 | Oxic | Silica Solubility at a Minimum | 31 |
| pH Buffers | High $SiO_2$ | 1-9 | Oxic | Minimal Corrosion | 23 |
| pH Buffers | High $SiO_2$ | 9-13 | Oxic | Active Corrosion | 23 |
| pH Buffers | Low $SiO_2$ | 1-3 | Oxic | Active Corrosion | 23 |
| pH Buffers | Low $SiO_2$ | 3-9 | Oxic | Minimal Corrosion | 23 |
| pH Buffers | Low $SiO_2$ | 9-13 | Oxic | Active Corrosion | 23 |
| DI Water | Waste | ? | Slight Anoxic | Surface Layer Enriched in Fe and Si | 40 |
| Basaltic Groundwater | Waste | 9.75 | Anoxic | Layer Formation Retarded Minimal Corrosion, Immunity (?) | 22 |
| Basaltic Groundwater | Waste | 9.75 | Anoxic | Corrosion < Oxic-Immunity (?) | 21 |
| Granitic Groundwater | Waste | ~8.5 | Anoxic | Corrosion < Oxic-Immunity (?) | 21 |
| DI Water+Fe° | Waste | 8 | Anoxic | Layer Formation Retarded Immunity (?) | 37 |

* SLS = Soda-Lime-Silica glass.

Borosilicate nuclear waste glasses contain aluminum, iron, and other transition metal cations. Iron is the predominant transition metal cation and can be present in both the oxidized and the reduced state. [11,12] The Eh-independent boundary between $Fe^{+++}$ (as $Fe(OH)^{++}_{aq}$) [2] and $Fe(OH)_3$ at log $C=10^{-4}M$ is proposed as the region of surface layer passivation for glasses containing iron (Figure 3a,b). This is based on the predominant role of $Fe(OH)_3$ in the surface layers of nuclear waste glasses [24,31]. This boundary occurs at pH values of 3-4 depending on log C and is in agreement with the observations of Wicks [26] that surface layers do not form on nuclear waste glasses at pH values <3. The activity-pH plot derived by Grambow [31] for commercial waste glasses demonstrates that $Fe(OH)_3$ is the dominatnt species precipitating between pH values of 7 and 9. Similar stability fields can be calculated and plotted on glass-specific Pourbaix diagrams for aluminum [5,44] or aluminosilicate complexes [35], zirconium [36], zinc [31] or any other metal hydroxide species mechanistically found to participate in the formation of surface layers.

Glasses such as borosilicate nuclear waste glasses, tektites, basalt and obsidians contain multivalent metal oxide species such as $Fe^{+2}/Fe^{+3}$ and $Mn^{+2}/Mn^{+3}$ which behave differently in oxidizing and reducing aqueous environments. Metal hydroxides such as $Mn(OH)_3$ and $Fe(OH)_3$ are expected to form from glasses containing $Mn_2O_3$ or $Fe_2O_3$ in oxidizing environments or by oxidative dissolution of MnO or FeO in oxidizing environments. The thermodynamic boundary between $Fe^{+++}$ (as $Fe(OH)^{++}$) and $Fe(OH)_3$ has already been defined as representing the Eh-independent portion of the surface passivation boundary. The thermodynamic boundary between $Fe^{++}$ and $Fe(OH)_3$ is, therefore, defined as the Eh-pH dependent extension of the surface passivation boundary for reduced glasses which undergo oxidative dissolution in oxidizing aqueous environments (Figure 3b).

Metal hydroxides such as $Mn(OH)_2$ and $Fe(OH)_2$ are stable in reducing aqueous environments [2] and would be expected to form from glasses containing MnO or FeO which are dissolved in anoxic (reducing) solutions. In the presence of silica, $Mn^{+2}$ or $Fe^{+2}$ silicate species are also stable in reducing environments. During dissolution of silicate glass in the presence of $Fe^{\circ}$ and aqueous $Fe^{+2}$, formation of a hydrated ferrous iron silicate complex, greenalite, was identified coexisting with $Fe(OH)_3$ [37]. The identification of this phase was consistent with the measured Eh-pH conditions and coincided with the thermodynamically calculated boundary between a ferrous iron silicate "$FeSiO_3$" and $Fe(OH)_3$ [37]. The formation of an anhydrous ferrous iron silicate complex is predicted by Garrels and Christ [2] in the presence of $Fe^{+2}$ and amorphous silica. However, greenalite is the hydrated analogue, $Fe_6Si_4O_{10}(OH)_8$. This same phase assemblage has been identified as the primary species responsible for the formation of iron ore deposits which form from iron-enriched silica solutions [38]. The iron ore silicate solutions are assumed [38] to be about $10^{-4}$ M $H_2SiO_3$ because that value represents the concentration of dissolved silica in equilibrium with quartz and clay mineral species [39].

Measured thermodynamic data is not available for greenalite. Klein and Bricker [38] calculated the free energy of formation for this phase to calculate an Eh-pH diagram for iron-ore formation. Using the data of Klein and Bricker [38] for greenalite in equilibrium with $H_2SiO_3$ at $10^{-4}$M, the Eh-dependent thermodynamic boundary between greenalite/$Fe(OH)_3$ is calculated and shown in Figure 3b. ($H_2SiO_3 = 10^{-4}$M is the same concentration used to define the $H_2SiO_3/HSiO_3^-$ boundary). The "$FeSiO_3$"/$Fe(OH)_3$ boundary previously calculated by Jantzen [37] in the presense of amorphous $SiO_2$ is shown for reference.

Because of the estimation of the thermodynamic data for greenalite, the exact boundary can vary between the two calculated boundaries shown on Figures 2 and 3. The greenalite/$Fe(OH)_3$ boundary is chosen to represent a change in the type of surface layer passivation, e.g. from hydroxide to silicate (Table 1) [22,40]. However, this may also represent a change in mechanism from surface passivation in oxidizing environments to immunity in reducing environments. If $Fe^{+2}$ in a reduced glass is structurally associated in the glass as an "$FeSiO_3$" component, then in the absence of oxygen there is no driving force for the dissolution of the iron silicate component. Likewise, in the presence of silica-saturated groundwaters, there is no driving force for the dissolution of silica and ferrous iron silicates would be thermodynamically stable. This has been observed in nature for basalts (composed of ferrous iron silicate minerals and up to 60 volume percent ferrous iron intergranular glass) that have existed for millions of years under reducing groundwater conditions. Laboratory experiments [22] with partially reduced borosilicate glasses in reducing groundwaters have demonstrated the immunity of these glasses under these environmental conditions (Table 1).

## CONCLUSIONS

A Pourbaix diagram can be derived for glass dissolution. The durability of over 300 high- and low-silica glasses can be predicted from hydration thermodynamics (from glass composition and solution pH) and used to quantify the Pourbaix diagram. The diagram can be quantified because of the colinearity of the hydration free energy with solution pH theoretically predicted (by the Nernst equation) and experimentally verified [7]. The Pourbaix diagram can also be quantified from the experimentally determined concentration-pH relations because of the colinearity of the hydration free energy and the solution concentrations determined by the pH dependence of the ion activities of the silicon and boron species.

The contribution of the glass compositon to the surface layer formation is fundamentally accounted for in the calculation of the hydration free energy from glass composition because (1) all glasses have some type of surface layer formation [30], (2) the type of surface layer formation is a function of the glass composition [30], and (3) the types of surface layers correlate with hydration free energy [5]. Because of the relationship of the free energy to the activities of all the species in a glass, the hydration free energy calculates the relative roles of amorphous silica dissolution as modified by surface layer formation. The data support the hypothesis of Grambow [15,16] that the dissolution of all silicate-based glasses can be described by the activity diagrams for the dissolution of amorphous silica.

The Pourbaix diagram construction demonstrates that the groundwaters of potential nuclear waste repositories center near the pH-Eh region of aqueous "absolute neutrality", e.g. $[OH^-] = [H^+]$ and $2pO_2 = pH_2$ [1]. The response of borosilicate waste glass to these groundwaters is quantified as a function of the solution pH since release of silicon and boron from nuclear waste glass is Eh-independent [21,22]. The anticipated groundwater conditions are found to be in the region of glass surface passivation and/or thermodynamic immunity.

The basalt, tuff, and granite groundwaters are all silica saturated. The concentration of $H_2SiO_3$ in GR-4 basalitic groundwater is $1.6 \times 10^{-3}$ M and can be as high as $2.6 \times 10^{-3}$ M [21] while the concentration of silicon in J-13 tuffaceous groundwater is $\sim 1 \times 10^{-3}$ M. The concentration of $H_2SiO_3$ in Stripa granitic groundwater is $\sim 4.3 \times 10^{-4}$ M [21]. The $H_2SiO_3/HSiO_3^-$ boundary is calculated for $H_2SiO_3 = 10^{-4}$ M. Higher concentrations of $\sim 10^{-3}$ move the $H_2SiO_3/HSiO_3^-$ active corrosion boundary to higher pH values. In other words, glass dissolution at higher pH values can be minimal in silica saturated groundwaters depending on the concentration of silica present. This may not be true of brines because the silica concentration is low and the ionic strength is high (solubility concentrations are dependent on the ionic strength of the solution).

Radioactive waste glass fabricated under reducing conditions and subsequently exposed to alkaline or neutral reducing groundwaters in the candidate geologic repositories (all the repository Eh conditions [7] fall below $2pO_2 = pH_2$) are anticipated to survive the oxygen-free subsurface environments for millions of years. Alteration should be minimal by analogy with the survival of natural mineral species and intergranular basaltic glasses (formed under high-temperature reducing conditions) which have been in contact with sub-surface groundwaters for millions of years [10].

In conclusion, a consistent Pourbaix diagram for nuclear waste glass can be described to unify the effects of repository specific Eh and pH conditions on glass durability. Known Eh-pH relationships can also be used to understand radionuclide solubility and the effects of glass/metal/groundwater interactions under different Eh-pH conditions.

## ACKNOWLEDGEMENTS

The information contained in this article was developed during the course of work under Contract No. DE-AC09-76SR00001 with the U.S. Department of Energy.

REFERENCES


1. M. Pourbaix, "Atlas of Electrochemical Equilibria in Aqueous Solutions", Eng.Trans. by J.A.Franklin, NACE,Houston, TX,644p (1974).
2. R.M. Garrels and C.L. Christ "Solutions, Minerals and Equilibria" Harper and Row, NY, 435pp (1965).
3. M.J Plodinec, C.M. Jantzen, and G.G. Wicks, Adv. in Ceramics, V.8, G.G. Wicks and W.A. Ross (Eds.), Am. Ceram.Soc., Columbus, OH, 491 (1984).
4. M.J. Plodinec, C.M. Jantzen and G.G. Wicks, Sci. Basis for Nucl. Waste Mgt., VII, G.L. McVay (Ed.), North-Holland, NY,755(1984).
5. C.M. Jantzen and M.J. Plodinec, J. Non-Cryst. Solids, 67, 207 (1984).
6. C.M. Jantzen, Adv. in Ceramics, V.20, D.E. Clarke, et. al.(Eds.) Am. Ceram. Soc., Columbus, OH, 703 (1986).
7. C.M. Jantzen, "Nuclear Waste Glass Durability: I. Predicting Environmental Response from Thermodynamic (Pourbaix) Diagrams", DP-MS-87-2, J. Am. Ceram. Soc. (in press).
8. M. Blumer, Helv. Chim. Acta, 33,1568 (1950).
9. W.C. Krumbein and R.M. Garrels, J. Geology, 60, 1 (1952).
10. R.M. Garrels "Geology" in Reference 1, p.89 (1974).
11. D.F. Bickford and R.B. Diemer, Jr., J. Non-Cryst. Solids, 84, 276 (1986).
12. D.F. Bickford, R.B. Diemer, Jr. and D.C. Iverson, ibid, 285 (1986).
13. D.Cooke and A.Paul, J. Br. Ceram.Soc., 77, 104 (1978).
14. A. Paul, J. Mat. Sci., 12, 2246 (1977).
15. B. Grambow, Adv. in Ceramics, V.8, G.G. Wicks and W.A. Ross (Eds.), Amer. Ceram. Soc.,Columbus, OH, 474 (1984).
16. B. Grambow and D.M. Strachan, Sci. Basis for Nucl. Waste Mgt., VII, G.L.McVay (Ed.) North-Holland, New York, 623 (1984).
17. P.W. Reimus,W.L. Kuhn,R.D. Peters,B.A. Pulsipher, PNL-5919 (1986).
18. R.G. Newton and A. Paul, Glass Technology, 21[6], 307 (1980).
19. C.M. Jantzen "Stability of Radioactive Waste Glasses in Groundwaters Assessed from Hydration Thermodynamics" (in preparation).
20. J.E. Mendel (compiler), U.S. DOE Report DOE/TIC-11400 (1981).
21. C.M. Jantzen and N.E. Bibler Sci. Basis for Nucl. Waste Mgt.,IX, L.O.Werme (Ed.), Mat. Res. Soc., Pittsburgh, PA, 219 (1986).
22. C.M. Jantzen and G.G. Wicks, Sci. Basis for Nucl. Waste Mgt. VIII, C.M.Jantzen et al (Eds.), Mat. Res. Soc., Pittsburgh, PA, 29 (1985).
23. P.B. Adams, J. Non-Cryst. Solids, 67, 193 (1984).
24. G.G. Wicks, W.C. Mosley, P.G. Whitkop, and K.A. Saturday, J. Non-Cryst. Solids, 49, 413 (1982).
25. D.E. Clark and L.L. Hench, Nucl. Chem. Waste Mgt., 2, 93 (1981).
26. G.G. Wicks, P.E. O'Rourke and P.G. Whitkop, DP-MS-81-104 (1982).
27. J.M. Horn, Jr. and G.Y. Onada, Jr., J. Am. Ceram. Soc., 61, 523 (1978).
28. C.Q. Buckwalter and L.R. Pederson, J. Am. Ceram. Soc., 65[9],431(1982).
29. A. Paul and M.S. Zaman, J. Mat. Sci., 13, 1499 (1978).
30. L.L. Hench and D.E. Clark, J. Non-Cryst. Solids, 28, 83 (1978).
31. B.Grambow, Sci. Basis for Nucl. Waste Mgt., V, W. Lutze (Ed.) North-Holland, New York, 93 (1982).
32. P.B. Macedo, Aa. Barkatt, B.C. Gibson, and C.J. Montrose, Nuclear Technology, 73, 199 (1986).
33. B.C. Sales, C.W. White, G.M. Begun, and L.A. Boatner, J. Non-Cryst. Solids, 67, 245 (1984).
34. C.M. Jantzen, D.R. Clarke, P.E.D. Morgan, and A.B. Harker, J. Am. Ceram. Soc., 65[6],292 (1982).
35. Aa. Barkatt, P.B. Macedo, W. Sousanpour, M.A. Boroomand, P. Szoke, and V.L. Rogers, PNL-4382 (1982).
36. C.R. Das, J. Am. Ceram. Soc., 64[4], 188 (1981).
37. C.M. Jantzen, Sci. Basis for Nucl. Waste Mgt. VII, G.L. McVay (Ed), Elsevier Publ., New York, 613 (1984).
38. C. Klein and O.P. Bricker , Econ. Geol., 73, 1457 (1977).
39. L. G. Sillen, Adv. in Chemistry Series, No. 67, 57-69 (1967).
40. A. Manara, F. Lanza, G. Ceccone, G. DellaMea, G. Salvagno, Sci. Basis for Nucl. Waste Mgt. VIII, C.M.Jantzen et.al (Eds.), Mat.Res.Soc., Pittsburgh, PA, 63 (1985).